Renormalization effects on MSSM from a calculable model of strongly coupled hidden sector

Masato Arai,[1,*] Shinsuke Kawai,[2,3,†] and Nobuchika Okada[4,‡]

[1] *Institute of Experimental and Applied Physics, Czech Technical University in Prague, Horská 3a/22, 128 00 Prague 2, Czech Republic*
[2] *Institute for the Early Universe (IEU), 11-1 Daehyun-dong, Seodaemun-gu, Seoul 120-750, Korea*
[3] *Department of Physics, Sungkyunkwan University, Suwon 440-746, Korea*
[4] *Department of Physics and Astronomy, University of Alabama, Tuscaloosa, AL35487, USA*

(Dated: November 25, 2010)

We investigate renormalization effects on the low energy mass spectrum of the minimal supersymmetric standard model (MSSM), using a calculable model of strongly coupled hidden sector. We model the hidden sector by $\mathcal{N}=2$ supersymmetric quantum chromodynamics with gauge group $SU(2)\times U(1)$ and $N_f=2$ matter hypermultiplets, perturbed by a Fayet-Iliopoulos term which breaks the supersymmetry down to $\mathcal{N}=0$ on a meta-stable vacuum. The hidden sector Kähler metric is renormalized, contributing to the MSSM renormalization group flows via gauge mediation. In contrast to perturbative examples of hidden sector renormalization studied in the literature, we find that our strongly coupled model exhibits rather intricate effects on the MSSM soft scalar mass spectrum, depending sensitively on how the hidden sector fields are coupled to the messenger fields. This model provides a concrete example in which the low energy spectrum of MSSM particles that are expected to be accessible in collider experiments can be directly computed using strongly coupled hidden sector dynamics.

I. INTRODUCTION

In the near future high energy collider experiments such as in the Large Hadron Collider are expected to yield a wealth of data that help us understand physics beyond the Standard Model. If the idea of supersymmetry (SUSY) is correct, we should detect superparticles. Major theoretical challenges are then to understand the mediation mechanism of SUSY breaking and the structure of a hidden sector, from a set of information given in the form of low energy spectrum of superparticles.

The low energy mass spectrum of a particle theory model is computed by solving renormalization group (RG) equations. Recently it was pointed out that the hidden sector dynamics affects RG flows in the visible sector [1, 2], and thus the hidden sector can be made visible through carefully analyzing the low energy mass spectrum of new particles. Based on this, RG analysis was performed for the constrained minimal supersymmetric standard model (cMSSM) [3] and the gauge-mediated supersymmetry breaking (GMSB) [4] scenario, both considering a simple toy model of hidden sector described by superpotential,

$$W=\frac{\lambda}{3}X^3, \tag{1}$$

where X is the hidden sector field and λ the self coupling. In particular, it was found that the hidden sector effects can be crucial in determination of the next-lightest superparticle (NLSP) [4], with exciting implications in future collider experiments.

The simple model of hidden sector (1) employed in these analyses [3, 4] is a mere toy, in the sense that the SUSY is assumed to be broken via some unknown mechanism that gives rise to a non-vanishing expectation value of the hidden sector field; in a more complete theory a hidden sector with a spontaneous SUSY breaking mechanism needs to be implemented. In fact, a natural mechanism of SUSY breaking is believed to be a dynamical one [5], where SUSY is broken by non-perturbative effects (such as instanton corrections) as the non-renormalization theorem protects SUSY perturbatively. It is thus important to study non-perturbative effects in the hidden sector that may affect the RG flow of the minimal supersymmetric Standard Model (MSSM). The present paper is intended to provide a first step in this direction. As it is not easy to devise a full dynamical model, we shall focus on a spontaneous SUSY breaking model that can be incorporated in the RG analysis of the low energy mass spectrum. We shall use a hidden sector of perturbed Seiberg-Witten theory type where the duality and holomorphicity allow us to relate the strongly coupled dynamics of the hidden sector to the RG flow in MSSM. Concretely, we shall study a hidden sector having $\mathcal{N}=2$ SUSY and $SU(2)\times U(1)$ gauge group, with $N_f=2$ matter hypermultiplets perturbed by a Fayet-Iliopoulos (FI) term. This theory is certainly not UV complete due to the $U(1)$ part; we assume that the theory is embedded in some UV complete theory and our description of the hidden sector is valid below the scale of the Landau pole. The effect of the FI term is to break the SUSY while the duality is maintained. We shall focus on the GMSB scenario [6] that is favored due to the natural suppres-

*Electronic address: Masato.Arai(AT)utef.cvut.cz
†Electronic address: kawai(AT)skku.edu
‡Electronic address: okadan(AT)ua.edu

sion of flavor-changing neutral currents. In GMSB the hidden sector fields that couple to the messengers need to be MSSM gauge singlets. It turns out that our model is sufficiently non-trivial and has various intriguing features. For example, as we will see, the hidden sector contribution to the MSSM RG equations can be positive or negative, depending on possible couplings between the hidden sector and the messenger fields; this is in contrast to the toy model studied in [3, 4] where the hidden sector effects always render the soft scalar particles lighter.

The plan of the present paper is as follows. In the next section we start by describing the model of the hidden sector. In Section 3 we discuss the RG flow in GMSB and in particular the contribution from the hidden sector. We present our numerical results in Section 4, and conclude in Section 5 with comments. Technical details of the hidden sector computations based on the $\mathcal{N}=2$ dualities are collected in the Appendix.

II. STRUCTURE OF THE HIDDEN SECTOR

We describe in this section the hidden sector which is responsible for the SUSY breaking. The model we shall consider is the $\mathcal{N}=2$ supersymmetric $SU(2)\times U(1)$ gauge theory with two matter hypermultiplets Q and $\tilde{Q}$, perturbed by a FI term. The model exhibits a metastable vacuum in the Coulomb branch; we use this as the SUSY breaking sector that couples to the MSSM sector via gauge mediation. This type of SUSY breaking scenario is particularly appealing for phenomenological applications; the R-symmetry is spontaneously broken and the gauginos can obtain masses. Also, such a local minimum in a landscape is expected to be quite ubiquitous in a larger theoretical set up such as string theory. An essential feature of the model is that the strongly coupled dynamics can be calculable due to the $\mathcal{N}=2$ dualities. We shall heavily rely on the machinery developed by Seiberg and Witten [7, 8]. This particular type of theory has been studied extensively in [9–13].

A. Classical theory

We first define our classical hidden sector Lagrangian and analyze its classical vacuum. The classical theory of the $\mathcal{N}=2$ $SU(2)\times U(1)$ model was originally analyzed in [14]. We shall use index $i=1,2$ for the $U(1)$ and the $SU(2)$ gauge groups. The $SU(2)$ and $U(1)$ $\mathcal{N}=2$ vector multiplets can be written using the $\mathcal{N}=1$ vector superfields V_i and the adjoint chiral superfields A_i, as (V_2,A_2) and (V_1,A_1). Similarly, the matter hypermultiplets are written in terms of the $\mathcal{N}=1$ chiral superfields as $(Q^r_I,\tilde{Q}^I_r)$, where $r=1,2$ and $I=1,2$ are the flavor and the $SU(2)$ color indices (the latter suppressed below). The superfield strengths are $W_{i\alpha}=-\frac{1}{4}\overline{D}^2(e^{-V_i}D_\alpha e^{V_i})$, with α the spinor index. The classical Lagrangian of the hidden sector is given by

$$\mathcal{L}_{\rm hid} \;=\; \mathcal{L}_{\rm VM}+\mathcal{L}_{\rm HM}+\mathcal{L}_{\rm FI}\;, \tag{2}$$

where

$$\begin{aligned}\mathcal{L}_{\rm VM} \;=\;& \frac{1}{4\pi}{\rm Im}\left[{\rm Tr}\left\{\tau_{22}\left(\int d^4\theta A_2^\dagger e^{2V_2}A_2e^{-2V_2}\right.\right.\right.\\ &\left.\left.\left.+\frac{1}{2}\int d^2\theta W_2^2\right)\right\}\right]\\ &+\frac{1}{8\pi}{\rm Im}\left[\tau_{11}\left(\int d^4\theta A_1^\dagger A_1+\frac{1}{2}\int d^2\theta W_1^2\right)\right],\end{aligned} \tag{3}$$

$$\begin{aligned}\mathcal{L}_{\rm HM} \;=\;& \int d^4\theta\left(Q_r^\dagger e^{2V_2+2V_1}Q^r+\tilde{Q}_re^{-2V_2-2V_1}\tilde{Q}^{\dagger r}\right)\\ &+\;\sqrt{2}\left(\int d^2\theta\tilde{Q}_r\left(A_2+A_1\right)Q^r+h.c.\right),\end{aligned} \tag{4}$$

and

$$\mathcal{L}_{\rm FI}=\lambda\int d^2\theta A_1+h.c. \tag{5}$$

Our convention here is ${\rm Tr}(T^aT^b)=\frac{1}{2}\delta^{ab}$ for the $SU(2)$ generators T^a. The complex gauge couplings of the $SU(2)$ and the $U(1)$ gauge interactions are

$$\tau_{22}=\frac{\theta}{\pi}+\frac{8\pi i}{g^2},\qquad \tau_{11}=\frac{8\pi i}{e^2}. \tag{6}$$

When the FI term (5) is absent, the theory has a global symmetry $SU(2)_{\rm left}\times SU(2)_{\rm right}\times SU(2)_R\times U(1)$. The $U(1)$ charges of the hypermultiplets are normalized to be unity. Using the $SU(2)_R$ symmetry we have chosen a frame in which the FI term appears only as an F-term. The FI term coefficient λ is a complex number with mass dimension two, and is assumed to be small compared to the $SU(2)$ dynamical scale Λ; thus the exact low energy effective action from the $\mathcal{N}=2$ part is unaffected by the additional term. The FI term breaks the $SU(2)_R$ symmetry down to an abelian subgroup $U(1)_{R'}$, and accordingly the global symmetry of the theory is broken to $SU(2)_{\rm left}\times SU(2)_{\rm right}\times U(1)_{R'}\times U(1)_R$.

It is straightforward to find the classical potential from the above Lagrangian,

$$\begin{aligned}V_{\rm cl} \;=\;& \frac{1}{g^2}\,{\rm Tr}[A_2,A_2^\dagger]^2+\frac{g^2}{2}(q_r^\dagger T^aq^r-\tilde{q}_rT^a\tilde{q}^{\dagger r})^2\\ &+\;q_r^\dagger[A_2,A_2^\dagger]q^r-\tilde{q}_r[A_2,A_2^\dagger]\tilde{q}^{\dagger r}+2g^2|\tilde{q}_rT^aq^r|^2\\ &+\;\frac{e^2}{2}\left(q_r^\dagger q^r-\tilde{q}_r\tilde{q}^{\dagger r}\right)^2+e^2|\sqrt{2}\tilde{q}_rq^r+\lambda|^2\\ &+\;2\left(q_r^\dagger|A_2+A_1|^2q^r+\tilde{q}_r|A_2+A_1|^2\tilde{q}^{\dagger r}\right)\;,\end{aligned} \tag{7}$$

where A_2, A_1, q^r and $\tilde{q}_r$ are the scalar components of the corresponding chiral superfields. The minima of the potential are obtained by the stationarity condition of the potential. In the Higgs branch the $SU(2)\times U(1)$ symmetry is completely broken and the moduli is along

$$\begin{aligned}&A_1=A_2=0,\quad q^1=\begin{pmatrix}v\\0\end{pmatrix},\quad q^2=\begin{pmatrix}0\\v\end{pmatrix},\\ &\qquad\qquad \tilde{q}_1=\begin{pmatrix}\tilde{v}&0\end{pmatrix},\quad \tilde{q}_2=\begin{pmatrix}0&\tilde{v}\end{pmatrix}.\end{aligned} \tag{8}$$

The components refer to the $SU(2)$ color, and $v, \tilde{v} \in \mathbb{C}$ satisfy $v\tilde{v} = -\frac{\lambda}{2\sqrt{2}}$ from the stationarity condition. In this branch the classical scalar potential $V_{\rm cl}$ vanishes. Hence the SUSY is preserved in the Higgs branch.

In the presence of the FI term the Coulomb branch is lifted and the vacuum is not supersymmetric anymore. A vacuum in this branch is parametrized as

$$A_1 = a_1, \quad A_2 = \frac{1}{2}\begin{pmatrix} a_2 & 0 \\ 0 & -a_2 \end{pmatrix},$$
$$q^1 = \tilde{q}_1 = \begin{pmatrix} v \\ 0 \end{pmatrix}, \quad q^2 = \tilde{q}_2 = 0, \tag{9}$$

where $a_1, a_2, v \in \mathbb{C}$. One possible branch is parametrized by $z \in \mathbb{C}$, such that

$$A_2 + A_1 = \begin{pmatrix} \frac{a_2}{2} & 0 \\ 0 & -\frac{a_2}{2} \end{pmatrix} + \begin{pmatrix} a_1 & 0 \\ 0 & a_1 \end{pmatrix} \equiv \begin{pmatrix} 0 & 0 \\ 0 & z \end{pmatrix}.$$

In this case

$$v^2 = -\frac{2\sqrt{2}e^2\lambda}{4e^2 + g^2}, \tag{10}$$

from the stationarity conditions and the potential minima become

$$V = \frac{|\lambda|^2 e^2 g^2}{4e^2 + g^2}. \tag{11}$$

The SUSY is seen to be broken at tree-level by the non-zero FI parameter λ. The SUSY breaking scales are found to be

$$F_1 = -\frac{e^2 g^2 \lambda^\dagger}{4e^2 + g^2},$$
$$F_2 = \frac{4e^2 g^2 \lambda^\dagger}{4e^2 + g^2}. \tag{12}$$

B. Qunatum theory

The low energy dynamics including the quantum effects is described by the Wilsonian effective action $\mathcal{L}_{\rm eff}$. While obtaining such an effective action by direct path integral is an arduous task, in the $\mathcal{N} = 2$ supersymmetric theory it is possible to determine the exact form exploiting the duality and holomorphicity [7, 8]. Our strategy here is to make a full use of the $\mathcal{N} = 2$ technology by treating the FI term as perturbation. Accordingly, the perturbative parameter of mass dimension 2 is assumed to be small compared to the $SU(2)$ dynamical scale Λ, i.e. $\lambda \ll \Lambda^2$. Then it is possible to expand the low energy effective action of our theory around the $\mathcal{N} = 2$ result [12, 13],

$$\mathcal{L}_{\rm eff} = \mathcal{L}_{\rm SUSY} + \mathcal{L}_{\rm soft} + \mathcal{O}\big((\lambda/\Lambda^2)^2\big). \tag{13}$$

Ignoring the FI term the classical $SU(2) \times U(1)$ gauge symmetry is broken to $U(1)_c \times U(1)$ in the Coulomb branch except at the origin of the moduli $(a_1, a_2) = (0, 0)$. This $U(1)_c$ is the remnant of the $SU(2)$. The $U(1)$ part is not asymptotically free and we restrict our moduli to be below the Landau pole, $|a_1| \leq \Lambda_L$. Since the $U(1)$ and $SU(2)$ interact through coupling to the hypermultiplets, we also impose $|a_2| \leq \Lambda_L$. We shall consider Λ_L to be much larger than the $SU(2)$ dynamical scale Λ, and regard Λ_L as a cut off scale of our theory.

The $\mathcal{N} = 2$ part, discussed also in [12, 13] in detail, consists of the vector multiplets and the hypermultiplets, $\mathcal{L}_{\rm SUSY} = \mathcal{L}_{\rm VM} + \mathcal{L}_{\rm HM}$. The former contains the superfield A_1 for the $U(1)$ and A_2 for the unbroken abelian subgroup $U(1)_c$ of $SU(2)$. The Lagrangian is

$$\mathcal{L}_{\rm VM} = \frac{1}{8\pi}{\rm Im}\left[\int d^4\theta \frac{\partial \mathcal{F}}{\partial A_i} A_i^\dagger + \frac{1}{2}\int d^2\theta \tau_{ij} W^{\alpha i} W^j_\alpha\right], \tag{14}$$

where $\mathcal{F}$ is the $\mathcal{N} = 2$ prepotential depending on A_1, A_2, Λ, Λ_L, and

$$\tau_{ij} = \frac{\partial^2 \mathcal{F}}{\partial A_i \partial A_j}. \tag{15}$$

The repeated $i, j = \{1, 2\}$ are summed over. The effective Lagrangian for the hypermultiplets is

$$\begin{aligned}\mathcal{L}_{\rm HM} \;=\; &\int d^4\theta \Big(M_r^\dagger e^{2n_m V_{2D} + 2n_e V_2 + 2nV_1} M^r \\ &\quad + \tilde{M}_r e^{-2n_m V_{2D} - 2n_e V_2 - 2nV_1} \tilde{M}^{r\dagger} \Big) \\ &+ \sqrt{2}\Big\{ \int d^2\theta \tilde{M}_r (n_m A_{2D} + n_e A_2 + nA_1) M^r + h.c. \Big\},\end{aligned} \tag{16}$$

where V_{2D} and A_{2D} are the dual variables of V_2 and A_2, and M^r, $\tilde{M}_r$ are the chiral superfields representing quarks, monopoles and dyons that become light in the vicinity of the singular points. These BPS states have quantum numbers $(n_e, n_m)_n$, with n_e and n_m the electric and magnetic $U(1)_c$ charges, and n represents the $U(1)$ charge. Denoting the dual variables of a_1 and a_2 as

$$a_{1D} \equiv \frac{\partial \mathcal{F}}{\partial a_1}, \quad a_{2D} \equiv \frac{\partial \mathcal{F}}{\partial a_2}, \tag{17}$$

the masses of the BPS states are

$$M_{\rm BPS} = \sqrt{2}|n_m a_{2D} + n_e a_2 + n a_1|. \tag{18}$$

This coincides with the spectrum of the $\mathcal{N} = 2$ supersymmetric QCD with gauge group $SU(2)$ and $N_f = 2$, with the two hypermultiplet masses $m_1 = m_2 = \sqrt{2}a_1$. The equivalence is further justified and utilized in the Appendix. The soft term takes the same form as the classical FI term,

$$\mathcal{L}_{\rm soft} = \lambda \int d^2\theta A_1 + h.c. \tag{19}$$

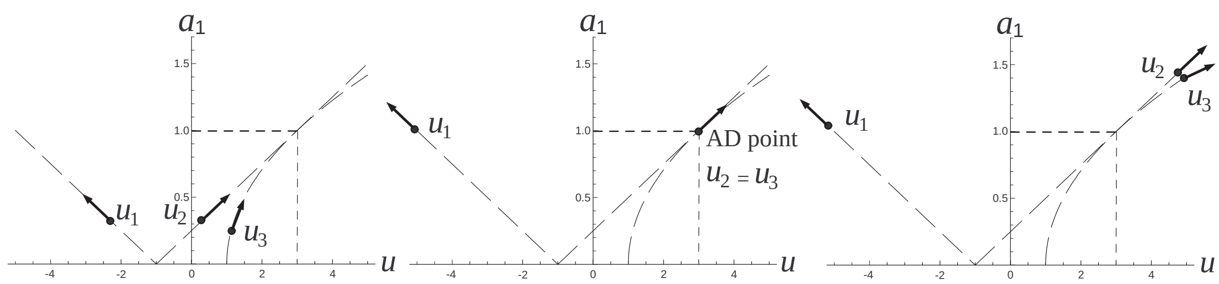

FIG. 1: The position of the singular points u_1, u_2, u_3 in the u-a_1 plane ($u \in \mathbb{R}$, $a_1 \in \mathbb{R}$ here and throughout the paper). We call u_1 the left dyon singular point, and u_2 the right dyon singular point. u_3 on the left panel is a monopole singular point, while on the right panel it is a quark singular point. The panel in the middle shows the Argyres-Douglas (AD) point where u_2 and u_3 coincide. Flows are shown as a_1 is increased. We have set $\Lambda = 2\sqrt{2}$.

C. The effective potential

The effective potential obtained from the effective Lagrangian (13) is

$$V_{\rm eff} = \frac{1}{2} b_{ij} D_i D_j + b_{ij} F_i F_j^\dagger + |F_M|^2 + |F_{\tilde{M}}|^2, \qquad (20)$$

where

$$b_{ij} = \frac{1}{8\pi} {\rm Im}\tau_{ij} \qquad (21)$$

is the Kähler metric (computed for appropriate local variables) and D_i, F_i, F_M, $F_{\tilde{M}}$ are the auxiliary fields for the superfields V_i, A_i, M, $\tilde{M}$. The effective potential depends on a_1 and a_2 as well as on the correct light degrees of freedom M and $\tilde{M}$. By solving the equations of motion the effective potential is written as,

$$\begin{aligned} V_{\rm eff} &= S\Big\{(M^r M_r^\dagger - \tilde{M}_r \tilde{M}^{r\dagger})^2 + 4|M^r \tilde{M}_r|^2\Big\} \\ &\quad +2T(M^r M_r^\dagger + \tilde{M}_r \tilde{M}^{r\dagger}) + U \\ &\quad -\frac{\sqrt{2} b_{12}}{\det b}\Big\{\lambda M_r^\dagger \tilde{M}^{r\dagger} + h.c.\Big\}, \end{aligned} \qquad (22)$$

with

$$\begin{aligned} S &= \frac{b_{11}}{2\det b}, \\ T &= |n_m a_{2D} + n_e a_2 + n a_1|^2, \\ U &= \frac{b_{22}|\lambda|^2}{\det b}. \end{aligned} \qquad (23)$$

The minima of the potential are found by solving the stationarity conditions for the fields M and $\tilde{M}$,

$$\begin{aligned} \frac{\partial V_{\rm eff}}{\partial M_r^\dagger} &= S\left\{2(|M|^2 - |\tilde{M}|^2)M^r + 4M^s \tilde{M}_s \tilde{M}^{r\dagger}\right\} \\ &\quad +2TM^r - \sqrt{2}\lambda \frac{b_{12}}{\det b} \tilde{M}^{r\dagger} = 0, \end{aligned} \qquad (24)$$

$$\begin{aligned} \frac{\partial V_{\rm eff}}{\partial \tilde{M}^{r\dagger}} &= S\left\{2(|\tilde{M}|^2 - |M|^2)\tilde{M}_r + 4M^s \tilde{M}_s M_r^\dagger\right\} \\ &\quad +2T\tilde{M}_r - \sqrt{2}\lambda \frac{b_{12}}{\det b} M_r^\dagger = 0, \end{aligned} \qquad (25)$$

where $|M|^2 = M^r M_r^\dagger$ and $|\tilde{M}|^2 = \tilde{M}_r \tilde{M}^{r\dagger}$. From (24) and (25),

$$(|M|^2 - |\tilde{M}|^2)\left[S(|M|^2 + |\tilde{M}|^2) + T\right] = 0, \qquad (26)$$

which implies

$$|M|^2 = |\tilde{M}|^2, \qquad (27)$$

as $T > 0$ except right at the singular points, and $S > 0$. Substituting this back into (24) and (25), the effective potential at the stationary points is found to be

$$V_{\rm min} = U - 4S|M|^4. \qquad (28)$$

The second term on the RHS represents condensation of the light BPS degrees of freedom that lower the potential from $V_{\rm min} = U$ (note that $S > 0$). The expectation value of the chiral fields is also found to be

$$|M|^2 = |\tilde{M}|^2 = \frac{1}{2S}\left\{\left|\frac{\lambda b_{12}}{\sqrt{2}\det b}\right| - T\right\}. \qquad (29)$$

The minima of the potential (28) is a functional of the BPS fields $M, \tilde{M}$ as well as the Kähler metric (21), which is found by an exact method detailed in the Appendix. As it turns out the theory is equivalent to $\mathcal{N} = 2$ supersymmetric quantum chromodynamics (QCD) with gauge group $SU(2)$ and $N_f = 2$ matter hypermultiplets having a common mass fixed by the $U(1)$ moduli parameter as

$m = \sqrt{2}a_1$. Potential minima appear at singular points where the light BPS degrees of freedom condensate. The location of the singular points are determined by a cubic curve [8]. There are 3 singular points apart from the one at the infinity, and they are parametrized by the $U(1)$ and $SU(2)$ moduli parameters a_1 and $u = \mathrm{Tr}(A_2^2)$. The 3 singular points $u = u_{1,2,3}$ as functions of a_1 and Λ are given by

$$u_1 = -\sqrt{2}a_1\Lambda - \frac{\Lambda^2}{8}, \quad u_2 = \sqrt{2}a_1\Lambda - \frac{\Lambda^2}{8}, \quad u_3 = 2a_1^2 + \frac{\Lambda^2}{8}. \tag{30}$$

If u and a_1 go off the real axes, V_{eff} starts to increase, moving away from the minima. As we are interested in physics near minima of the potential we shall be concerned with real values of u and a_1. Numerical study shows the following structure of singularities and the corresponding vacua for $u, a_1 \in \mathbb{R}$ (Figs.1 and 2; see also Fig.2 of [11]):

(1) $0 \leq \mathrm{Re}(a_1) < \frac{\Lambda}{2\sqrt{2}}$ – There are two dyon (u_1, u_2), and one monopole (u_3) singular points. The two dyon points give local potential minima (V^1_{min} and V^2_{min}), while the point u_3 does not correspond to a minimum of the potential. At $a_1 = 0$, u_1 (the left dyon) and u_2 (the right dyon) are degenerate and this type of vacua are analyzed in [15]. Note that the effective theory breaks down at the $a_1 = 0$ point and a direct analysis is difficult. Nevertheless, we know that $U > 0$ and it is unlikely that the instanton effects (the second term of (28)) cancel U exactly. Also, SUSY is broken at the tree level and it is unlikely that it is recovered by quantum effects. For these reasons it is natural to suppose that the potential minimum at coincident u_1 and u_2 is a SUSY breaking metastable vacuum. By dimensional analysis we assume $V_{\mathrm{min}} \sim \lambda^2$ at this point, which is small but non-zero. As a_1 is increased, the two potential minima increase but continue to be $V^1_{\mathrm{min}} = V^2_{\mathrm{min}}$ (Fig.2).

(2) $\mathrm{Re}(a_1) = \frac{\Lambda}{2\sqrt{2}}$ – This is the Argyres-Douglas (AD) point where u_2 and u_3 coincide. The effective theory description breaks down at this point.

(3) $\mathrm{Re}(a_1) > \frac{\Lambda}{2\sqrt{2}}$ – There are again 3 singular points. u_1 and u_2 are dyons, while u_3 is now a quark singular point. The minimum V^1_{min} continues to increase, while the minimum at the quark singular point V^3_{min} starts to decrease, giving a runaway vacuum at a_1, $u \to \infty$. u_2 does not correspond to a potential minimum in this region.

There are two possible SUSY vacua in the model: the first one is on the Higgs branch, and the other is the runaway vacuum on the Coulomb branch (although it is somewhat questionable to call the latter a SUSY vacuum since the theory is not well defined beyond the Landau pole). Clearly, V^3_{min} is almost zero in the runaway vacuum

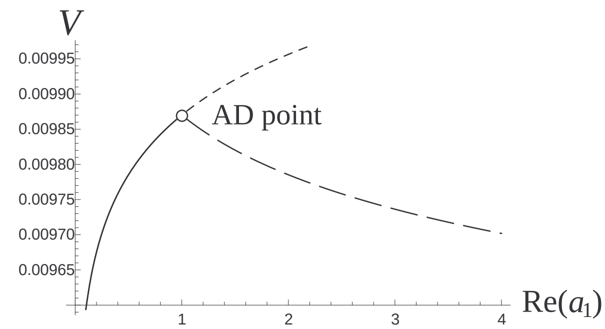

FIG. 2: The local minima of the scalar potential plotted against the flows of the singular points, for $a_1 \in \mathbb{R}$. The solid curve shows the minima of the potential along the two dyon singular points u_1 and u_2, which coincide for $0 \leq a_1 \leq \frac{\Lambda}{2\sqrt{2}}$. $a_1 = \frac{\Lambda}{2\sqrt{2}}$ corresponds to the AD point. When $a_1 > \frac{\Lambda}{2\sqrt{2}}$ the potential minimum for u_2 cease to exist, while u_1 (the dotted curve) continues to be a minimum with V^1_{min} increasing. The other branch (the dashed curve) is a potential minimum around the quark singular point u_3, which shows up for $a_1 > \frac{\Lambda}{2\sqrt{2}}$ and corresponds to a runaway vacuum. Here we set $\lambda = 0.1$ and $\Lambda = 2\sqrt{2}$.

as Λ_L is taken to be sufficiently large. We approximate the runaway vacuum to be at $a_1 \sim \Lambda_L$. The decay rate of the local potential minimum at $u_1 = u_2 = -\Lambda^2/8$, $a_1 = 0$ into these SUSY vacua is computed in [13]. The bounce action corresponding to the decay from the local minimum to the runaway vacuum is computed with triangle approximation [16–18], as

$$B \sim \frac{\Lambda_L^4}{\lambda^2}. \tag{31}$$

This is extremely large as the potential barrier is very wide. The bounce action to the Higgs vacuum at $a_1 = a_2 = 0$ and $q, \tilde{q} \sim \sqrt{\lambda}$ is estimated similarly. For $\Lambda = 2\sqrt{2}$ and $\lambda = 0.1$ we have $B \sim \mathcal{O}(10^6)$. In both decay channels the decay rate e^{-B} is extremely small, and hence the lifetime of the false vacuum is very large. Thus it is regarded as a metastable vacuum.

III. HIDDEN SECTOR RENORMALIZATION EFFECTS ON MSSM

The spontaneous SUSY breaking in the hidden sector is communicated to the visible sector via messenger fields, which, in the GMSB scenario we consider, couple to the MSSM fields through the standard gauge and gaugino interactions. After integrating out the messenger fields (i.e. below the messenger scale M_{m}), the interaction between the hidden and the visible sectors is described by the Lagrangian,

$$\mathcal{L}_{\rm int} = k_i \int d^4\theta \frac{X^\dagger X}{M_{\rm m}^2}\Phi_i^\dagger \Phi_i + \left(w_a \int d^2\theta \frac{X}{M_{\rm m}} W^{a\alpha} W^a_\alpha + h.c. \right). \quad (32)$$

Here, X is an MSSM gauge singlet field in the hidden sector, Φ_i and W^a the MSSM superfields (the indices $i = \{Q, U, D, L, E, H_u, H_d\}$ and $a = \{1, 2, 3\}$ denote the MSSM chiral multiplets and the MSSM gauge groups $U(1)$, $SU(2)$, $SU(3)$, respectively). The coupling k_i is subject to wave function renormalizatoin of the hidden sector fields, while the non-renormalization theorem forbids w_a to be renormalized. In our model of the hidden sector there are multiple candidates for such X. Below we shall see that different choices of X lead to different types of contribution to the MSSM RG equations. Here and below we assume the minimal GMSB, with messenger fields belonging to $\mathbf{5} + \bar{\mathbf{5}}$ of an $SU(5)$ with the sum of the Dynkin indices $N_5 = 1$.

A. Gauge-mediated SUSY breaking

Let us first describe generic features of hidden sector contributions to the MSSM RG flow [2, 3], focusing on the GMSB scenario [4]. As SUSY is broken in the hidden sector the gauginos and scalars in the MSSM acquire masses through 1- and 2-loop corrections respectively (the 2nd and 1st terms in (32)). The gaugino masses at the messenger scale $\mu = M_{\rm m}$ are

$$M_a(t=0) = \frac{\alpha_a}{4\pi}\frac{\langle F_X \rangle}{M_{\rm m}}, \quad (33)$$

where $t = \ln(\mu/M_{\rm m})$, F_X is the F-term for the hidden sector field X, $\alpha_a = g_a^2/4\pi$ and g_a ($a = 1, 2, 3$) are the gauge couplings of $U(1)$, $SU(2)$, $SU(3)$. The soft scalar masses at the messenger scale are given by

$$m_i^2(t=0) = 2\left(\frac{\langle F_X \rangle}{M_{\rm m}}\right)^2 \sum_{a=1}^{3} C_2^a(R_i)\left(\frac{\alpha_a}{4\pi}\right)^2, \quad (34)$$

where $C_2^a(R_i)$ are the quadratic Casimir for the matter fields in representation R_i of the a-th MSSM gauge group. These masses generated at the messenger scale set boundary conditions of the RG flow. The A-terms at the messenger scale are set to be zero.

The coefficients k_i of (32) are renormalized by the MSSM gauge interactions and the wave function renormalization of the hidden sector fields, $X \to Z_X^{-\frac{1}{2}} X$. The flow is described by the RG equaions,

$$\frac{d}{dt}k_i(t) = \gamma(t) k_i(t) - \frac{1}{16\pi^2}\sum_{a=1}^{3} 8 C_2^a(R_i) g_a^6(t) G_a, \quad (35)$$

where

$$G_a \equiv w_a w_a^\dagger. \quad (36)$$

In the first term $\gamma(t)$ is the anomalous dimension at $t = \ln(\mu/M_{\rm m})$ arising from the hidden sector interaction (32), and the second term is the leading visible sector contribution. The RG equations are solved as

$$k_i(t) = k_i(0)\exp\left(-\int_t^0 dt' \gamma(t')\right) + \frac{1}{16\pi^2}\sum_{a=1}^{3} 8C_2^a(R_i)\int_t^0 ds\, g_a^6(s)\exp\left(-\int_t^s dt'\gamma(t')\right) G_a. \quad (37)$$

The evolution of the MSSM scalar masses now includes hidden sector contributions. In the leading order these masses are

$$m_i^2(t) = k_i(t)\left(\frac{\langle F_X\rangle}{M_{\rm m}}\right)^2, \quad (38)$$

with

$$k_i(0) = 2\sum_{a=1}^{3} C_2^a(R_i)\left(\frac{\alpha_a(M_{\rm m})}{4\pi}\right)^2. \quad (39)$$

The gauge couplings run according to the standard 1-loop formula,

$$\frac{1}{\alpha_a(\mu)} = \begin{cases} \dfrac{1}{\alpha_a(M_Z)} - \dfrac{b_a}{2\pi}\ln\dfrac{M_S}{M_Z} - \dfrac{b_a^S}{2\pi}\ln\dfrac{\mu}{M_S}, & (\mu > M_S) \\ \dfrac{1}{\alpha_a(M_Z)} - \dfrac{b_a}{2\pi}\ln\dfrac{\mu}{M_Z}, & (\mu \le M_S) \end{cases} \quad (40)$$

where $(b_1^S, b_2^S, b_3^S) = (-3, 1, 33/5)$ for the MSSM and $(b_1, b_2, b_3) = (-7, -19/6, 41/10)$ for the Standard Model gauge couplings. M_Z and $M_{\rm S}$ are the Z-boson mass and a typical soft mass scale, respectively.

The first term in (35) implies that the hidden sector renormalization contributes to the RG equations for the MSSM soft scalar masses as

$$\frac{dm_i^2}{dt} = \left.\frac{dm_i^2}{dt}\right|_{\rm MSSM} + \gamma(t) m_i^2. \quad (41)$$

Explicitly, the RG equations are

$$8\pi^2 \frac{dm_Q^2}{dt} = \xi_t + \xi_b - \frac{16}{3} g_3^2 M_3^2 - 3 g_2^2 M_2^2 - \frac{1}{15} g_1^2 M_1^2 + \frac{1}{5} g_1^2 \xi_1 + 8\pi^2 \gamma m_Q^2, \quad (42)$$

$$8\pi^2 \frac{dm_U^2}{dt} = 2\xi_t - \frac{16}{3} g_3^2 M_3^2 - \frac{16}{15} g_1^2 M_1^2 - \frac{4}{5} g_1^2 \xi_1 + 8\pi^2 \gamma m_U^2, \quad (43)$$

$$8\pi^2 \frac{dm_D^2}{dt} = 2\xi_b - \frac{16}{3} g_3^2 M_3^2 - \frac{4}{15} g_1^2 M_1^2 + \frac{2}{5} g_1^2 \xi_1 + 8\pi^2 \gamma m_D^2, \quad (44)$$

$$8\pi^2 \frac{dm_L^2}{dt} = \xi_\tau - 3 g_2^2 M_2^2 - \frac{3}{5} g_1^2 M_1^2 - \frac{3}{5} g_1^2 \xi_1 + 8\pi^2 \gamma m_L^2, \quad (45)$$

$$8\pi^2 \frac{dm_E^2}{dt} = 2\xi_\tau - \frac{12}{5} g_1^2 M_1^2 + \frac{6}{5} g_1^2 \xi_1 + 8\pi^2 \gamma m_E^2, \quad (46)$$

$$8\pi^2 \frac{dm_{H_u}^2}{dt} = 3\xi_t - 3 g_2^2 M_2^2 - \frac{3}{5} g_1^2 M_1^2 + \frac{3}{5} g_1^2 \xi_1 + 8\pi^2 \gamma m_{H_u}^2, \quad (47)$$

$$8\pi^2 \frac{dm_{H_d}^2}{dt} = 3\xi_b + \xi_\tau - 3 g_2^2 M_2^2 - \frac{3}{5} g_1^2 M_1^2 - \frac{3}{5} g_1^2 \xi_1 + 8\pi^2 \gamma m_{H_d}^2, \quad (48)$$

where

$$\xi_t = y_t^2 (m_{H_u}^2 + m_Q^2 + m_U^2 + A_t^2), \quad (49)$$

$$\xi_b = y_b^2 (m_{H_d}^2 + m_Q^2 + m_D^2 + A_b^2), \quad (50)$$

$$\xi_\tau = y_\tau^2 (m_{H_d}^2 + m_L^2 + m_E^2 + A_\tau^2), \quad (51)$$

and

$$\xi_1 = \frac{1}{2} \left\{ m_{H_u}^2 - m_{H_d}^2 + \mathrm{Tr}(m_Q^2 - 2m_U^2 + m_D^2 + m_E^2 - m_L^2) \right\}. \quad (52)$$

The trace here means sum over the generations. Within our approximation only the $(3,3)$ family component of the three Yukawa matrices, y_t, y_b, y_τ, are set to be non-zero. The corresponding non-zero components of the three trilinear A-term matrices are A_t, A_b, A_τ.

The above equations for the squarks and sleptons apply to the 3rd family; the equations for the 1st and the 2nd families are obtained from above by discarding the Yukawa and the A-term contributions (i.e. setting the ξ_t, ξ_b, ξ_τ terms to be zero). All the other RG equations (the gauge couplings, the gaugino masses, the Yukawa couplings and the A-terms) are not affected by the hidden sector and are given e.g. in [19].

B. The models of hidden-visible couplings

In the preceding section we described the $\mathcal{N} = 2$ supersymmetric $SU(2) \times U(1)$ gauge theory with $N_f = 2$ matter hypermultiplets. Now let us use this as the hidden sector and discuss how it can affect the RG flow of the MSSM sector within the GMSB scenario. There are 3 singular points in the hidden sector as shown in Fig.1. Their positions in the a_1-u moduli space are given by (30). As energy scale changes the singular points move on the a_1-u plane. The RG flow in the hidden sector is understood as a flow in the a_1-u plane. A natural choice of RG flow in a multidimensional moduli space is along a trough of potential [20, 21]. In our model there are two possible troughs: one along the left dyon singularity, and the other along the quark singularity connected to the right dyon singularity below the AD point. We shall analyze RG flows along the singular points u_1 and u_2 from UV (Fig.3), as both u_1 and u_2 flow to the SUSY breaking vacuum in the IR. Along these flows, u_1 and u_2 are related to a_1 by (30) and renormalized quantities such as the gauge coupling constant are all functions of a_1. We will choose a_1 as the renormalization scale and identify it with μ in the RG analysis, with appropriate rescaling.

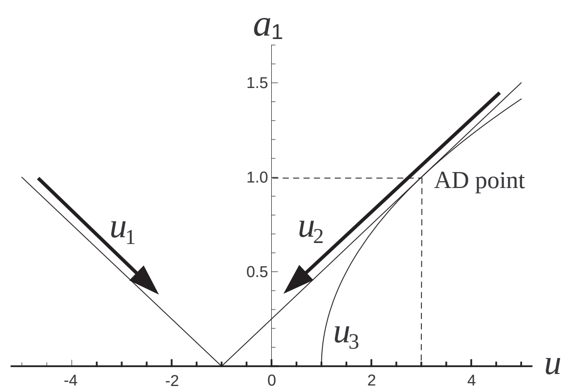

FIG. 3: Flows of potential minima along the two dyon singular points.

The messenger fields Ψ and $\tilde{\Psi}$ charged under the MSSM gauge groups may couple to the hidden sector fields in various ways. We consider the following 2 cases:

(1) Coupling to A_1 – We choose the superpotential of the messenger fields Ψ, $\tilde{\Psi}$ as

$$W_{\rm mess} = A_1 \Psi\tilde{\Psi} + M_{\rm m}\Psi\tilde{\Psi}. \qquad (53)$$

Here, $M_{\rm m}$ is the messenger mass which is taken to be 10^{13} GeV in the numerics. The hidden sector field X is A_1 and its boundary condition at the SUSY breaking vacuum is $\langle X\rangle = \langle A_1\rangle = 0$. The breaking scale is $\langle F_1\rangle \sim \lambda$.

(2) Coupling to A_2 – The messenger superpotential is

$$W_{\rm mess} = \frac{u}{M_{\rm c}}\Psi\tilde{\Psi} + M_{\rm m}\Psi\tilde{\Psi}, \qquad (54)$$

where $M_{\rm m}$ is the messenger mass as above, and $u = {\rm Tr}(A_2^2)$. The mass scale $M_{\rm c}$ has been introduced since u is a higher dimensional operator. The hidden sector field is $X = u/M_{\rm c}$. The boundary condition at the SUSY breaking vacuum is $\langle u\rangle = -\Lambda^2/8$. The breaking scale is $\langle F_2\rangle \sim \lambda$.

Note that $\langle X\rangle$ is much smaller than $M_{\rm m}$ and does not affect the GMSB boundary conditions (33), (34). The hidden sector field X undergoes wave function renormalization as $X \to Z_X^{-1/2}X$. The anomalous dimension is written using the coefficient Z_X as

$$\gamma(t) = -n_X \mu\frac{d}{d\mu}\ln Z_X = -n_X\frac{d}{dt}\ln Z_X, \qquad (55)$$

where n_X is the scaling dimension of the operator coupled to the messenger field ($n_X = 1$ for $X = A_1$ and $n_X = 2$ for $X = u/M_{\rm c}$). Using this in (37) we obtain,

$$\begin{aligned} k_i(t) &= k_i(0)\left(\frac{Z_X(0)}{Z_X(t)}\right)^{n_X} \\ &+\frac{1}{16\pi^2}\sum_{a=1}^{3} 8C_2^a(R_l)\int_t^0 ds g_a^6(s)\left(\frac{Z_X(s)}{Z_X(t)}\right)^{n_X} G_a. \end{aligned} \qquad (56)$$

The wave function renormalization is induced by change of the Kähler metric in the hidden sector. The coefficient Z_X is identified with b_{ij} of (21). In the A_1-coupled case for example,

$$Z_{A_1} = \frac{\partial^2 K}{\partial A_1 \partial A_1^\dagger} = \frac{1}{8\pi}{\rm Im}\frac{\partial^2}{\partial A_1\partial A_1^\dagger}\left(\frac{\partial \mathcal{F}}{\partial A_1}A_1^\dagger\right) = b_{11}. \qquad (57)$$

Similarly, in the A_2-coupled case we have $Z_{A_2} = b_{22}$. While the semiclassical picture is only applicable in the UV regions, we can follow the RG flow down to IR since b_{11} and b_{22} are globally solved using the exact method.

IV. NUMERICAL RESULTS

In this section we analyze the RG flows of the MSSM scalar masses for the models (53) and (54). We solve the RG equations (42)-(48) numerically along the two possible flows u_1 and u_2 of Fig.3. The coupling to the hidden sector affects the MSSM RG flows between the messenger scale $\mu = M_{\rm m}$ and the hidden sector scale $\mu = M_{\rm hid}$, through the anomalous dimension $\gamma(t)$. We first evaluate the anomalous dimension (55) and the wave function renormalization scale (57). We follow the conventions of Sec. II C and set the dynamical scale to be $\Lambda = 2\sqrt{2}$, and then rescale it in order to suit the minimal GMSB scenario with high messenger scale.

In our numerical calculations we made following approximations that are standard in the GMSB RG analysis: only the $(3,3)$ family component of the three Yukawa matrices, and only the $(3,3)$ family component of the trilinear A-term matrices, are set to be non-zero. The latter are assumed to vanish at the messenger scale. We use following values: $\tan\beta = 10$, the soft mass scale $M_S = 500$ GeV, and the messenger scale $M_{\rm m} = 10^{13}$ GeV. The hidden sector scale is $M_{\rm hid} = \langle F_X\rangle^{1/2} = 10^9$ GeV, above which the hidden sector degrees of freedom are integrated out.

A. A_1-coupled messenger

1. Flow along the left dyon singularity

Along the flow u_1, the wave function renormalization scale and the anomalous dimension are

$$Z_{A_1} = b_{11}(u_1(a_1), a_1)\Big|_{a_1=\mu}, \qquad (58)$$

$$\gamma_{A_1} = -a_1\frac{d}{da_1}Z_{A_1}(u_1(a_1), a_1)\Big|_{a_1=\mu}. \qquad (59)$$

In Fig.4 we show numerical plots of (58) and (59) along the renormalization scale μ, with $\Lambda = 2\sqrt{2}$. In the phenomenological setting we rescale $\mu \to (10^9/\tilde{M}_{\rm hid})\mu$, where $\tilde{M}_{\rm hid} = 0.2$ is the hidden scale before rescaling[1]. The RG equations (42)-(48) are then solved numerically, using the anomalous dimension (59) with the rescaled μ. The results are shown in Fig.5 for the slepton and squark masses, with and without the hidden sector effects. For both sleptons and quarks, the hidden sector effects are seen to decrease the masses, as the scale goes down from the messenger to the hidden scale. This behavior is understood by looking at Eqn. (56). The effects of the hidden sector come in $Z_X(0)/Z_X(t)$ and $Z_X(s)/Z_X(t)$. The contribution from the latter (the 2nd term of (56)) is suppressed by the gauge coupling constants, and thus the dominant contribution is from the former (the 1st term). We see from Fig.4 that $Z_{A_1}(0)/Z_{A_1}(t) < 1$, leading to the smaller masses of Fig.5.

[1] For $\tilde{M}_{\rm hid} \lesssim 0.2$ the condensations (29) around the left and right dyon points overlap, signaling the breakdown of the local low energy effective theory description. For this reason we shall adopt $\tilde{M}_{\rm hid} = 0.2$ when analyzing the left dyon singularity, also in the A_2-coupled model below.

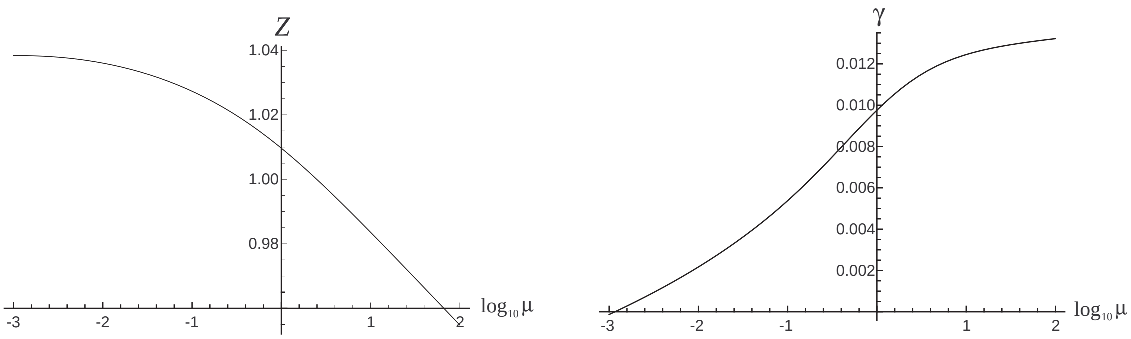

FIG. 4: The wave function renormalization coefficient $Z = b_{11}$ (left) and the anomalous dimension γ (right) along the flow u_1 in the A_1-coupled model.

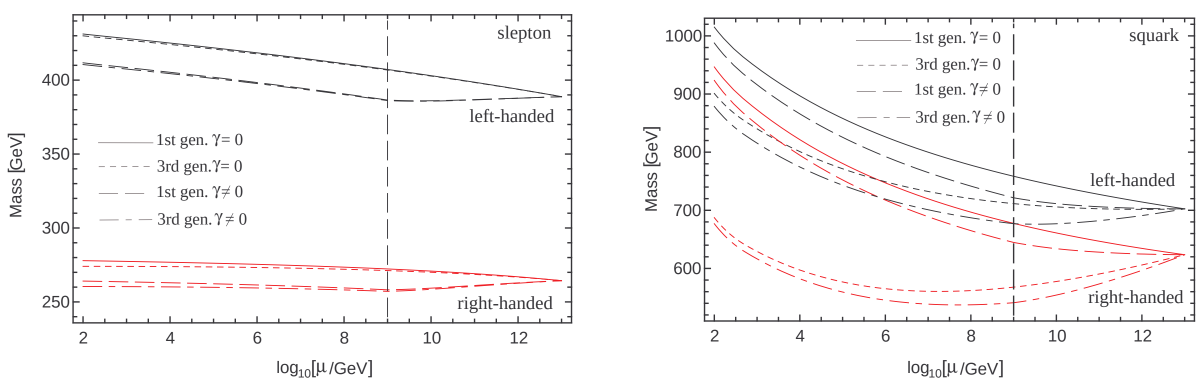

FIG. 5: The mass RG flows for the 1st and 3rd generation sleptons (the left panel) and squarks (right panel), with $(\gamma \neq 0)$ and without $(\gamma = 0)$ hidden sector effects. Here, the messenger is coupled to A_1, and γ is the anomalous dimension for A_1 shown in Fig.4. The flow is taken along the u_1 (left dyon) singularity. We have rescaled $\mu \to (10^9/\tilde{M}_{\rm hid})\mu$, where $\tilde{M}_{\rm hid} = 0.2$ is the hidden scale before rescaling. We have chosen $M_{\rm hid} = 10^9$ GeV (the vertical dashed line), $M_{\rm m} = 10^{13}$ GeV, and $\tan\beta = 10$.

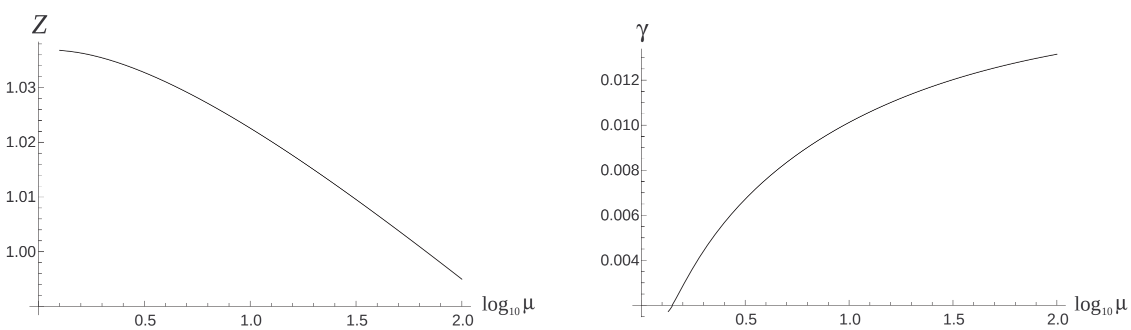

FIG. 6: The wave function renormalization coefficient $Z = b_{11}$ (left) and the anomalous dimension γ (right) along the flow u_2 in the A_1-coupled model.

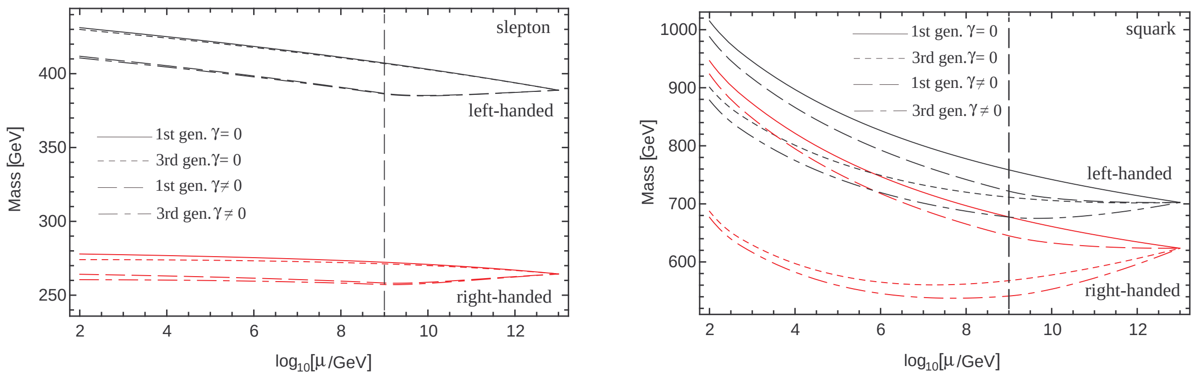

FIG. 7: The mass RG flows for the 1st and 3rd generation sleptons (the left panel) and squarks (right panel), with ($\gamma \neq 0$) and without ($\gamma = 0$) hidden sector effects. The vertical dashed line indicates the hidden scale $M_{\rm hid} = 10^9$ GeV. The messenger is coupled to A_1 and the flow is taken along the u_2 (right dyon) singularity. We have rescaled $\mu \to (10^9/\tilde{M}_{\rm hid})\mu$, where $\tilde{M}_{\rm hid} = 1.2$. We have chosen $M_{\rm m} = 10^{13}$ GeV and $\tan\beta = 10$.

2. Flow along the right dyon singularity

We next consider the RG flows of the MSSM scalar masses along u_2. In this case, the flow is somewhat complicated as it contains the AD point. At the AD point ($\mu = a_1 = 1$ in our scale $\Lambda = 2\sqrt{2}$) the theory becomes superconformal and the local effective theory description breaks down. In our analysis we set the hidden scale to be $\tilde{M}_{\rm hid} = 1.2$, i.e. above the AD point so that the hidden sector dynamics at the AD point does not contribute to the RG flow. In this case the wave function renormalization coefficient and the anomalous dimension are

$$Z_{A_1} = b_{11}(u_2(a_1), a_1)\Big|_{a_1=\mu}, \qquad (60)$$

$$\gamma_{A_1} = -a_1 \frac{d}{da_1} Z_{A_1}(u_2(a_1), a_1)\Big|_{a_1=\mu}. \qquad (61)$$

These are shown in Fig.6. Numerical solutions to the RG equations (42)-(48), with rescaling $\mu \to (10^9/\tilde{M}_{\rm hid})\mu$, are shown in Fig.7. We see from the messenger scale down to the hidden scale the hidden sector effects render both slepton and squark masses smaller. Like in the u_1 case, this is due to $Z_{A_1}(0)/Z_{A_1}(t) < 1$ in Eqn. (56).

B. A_2-coupled messenger

1. Flow along the left dyon singularity

Let us discuss the A_2-coupled mass RG flow (54). We first consider the flow along u_1. In this model, the wave function renormalization coefficient and the anomalous dimension are

$$Z_{A_2} = b_{22}(u_1(a_1), a_1)\Big|_{a_1=\mu}, \qquad (62)$$

$$\gamma_{A_2} = -2a_1 \frac{d}{da_1} Z_{A_2}(u_1(a_1), a_1)\Big|_{a_1=\mu}. \qquad (63)$$

These are shown in Fig.8. In contrast to the previous examples we see that Z_{A_2} increases as the scale goes up to $\mu = 1$ and monotonically decreases above that scale. Accordingly, γ_{A_2} changes its sign at $\mu = 1$. Fig.9 shows the mass RG flows of the sleptons and the squarks, obtained by setting $\mu \to (10^9/\tilde{M}_{\rm hid})\mu$ and $\tilde{M}_{\rm hid} = 0.2$. In this setting, we see that the hidden sector gives rise to different effects on the MSSM mass spectrum for $\mu > M'$ and $\mu < M'$, where $M' = 5 \times 10^9$ GeV is the energy scale corresponding to $\mu = 1$ before rescaling. When $M' < \mu < M_{\rm m}$, the effect of the hidden sector is to decrease the scalar masses, which is understood from (56) with $Z_{A_2}(0)/Z_{A_2}(t_{M'}) < 1$ (where $t_\mu \equiv \ln(\mu/M_m)$), the same effect as in the A_1-coupled model. For $\tilde{M}_{\rm hid} < \mu < M'$ the effect of the hidden sector increases the soft scalar masses, resulting from $Z(t_{M'})/Z(t_{M_{\rm hid}}) > 1$. In fact, the scale M' is considered to be a boundary between the weak and strong coupling regions. The messenger fields are coupled to $u/M_{\rm c}$, where $u = {\rm Tr}(A_2^2)$ semiclassically and A_2 is a good variable in the weak coupling region. We have extrapolated $Z_{A_2} = b_{22}$ down to the strong coupling region using the exact solution. Below the scale M' the nature of the coupling changes, leading to the increasing effect of the MSSM scalar masses.

2. Flow along the right dyon singularity

Finally we consider the A_2-coupled model along the flow u_2. As in the A_1-coupled case along u_2, we take

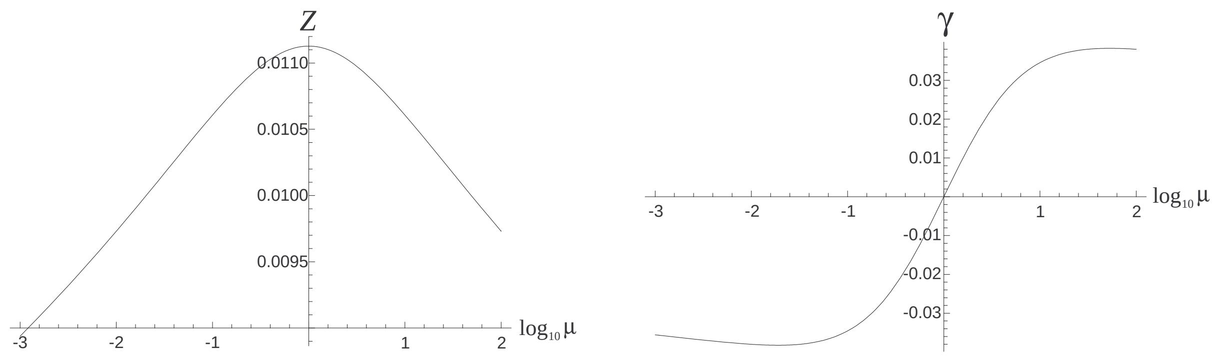

FIG. 8: The wave function renormalization coefficient $Z = b_{22}$ (left) and the anomalous dimension γ (right) along the flow u_1 in the A_2-coupled model.

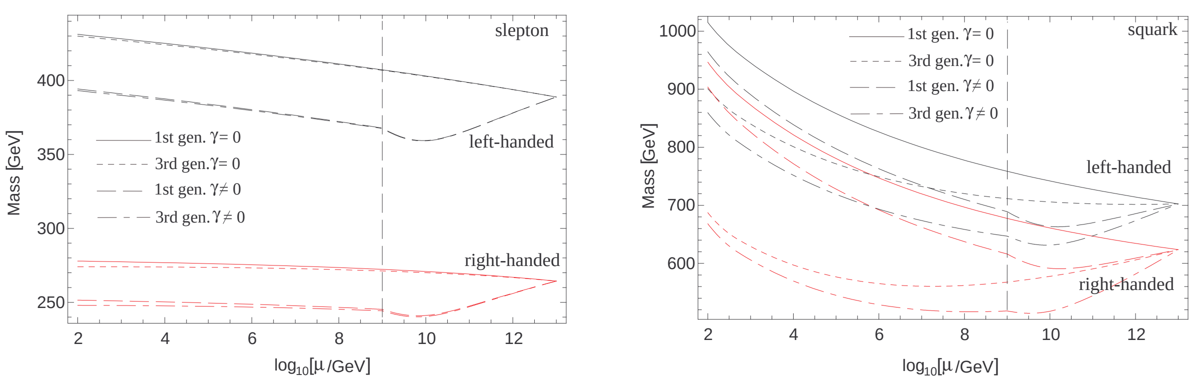

FIG. 9: The mass RG flows for the 1st and 3rd generation sleptons (the left panel) and squarks (right panel), with $(\gamma \neq 0)$ and without $(\gamma = 0)$ hidden sector effects. The vertical dashed line indicates the hidden scale $M_{\rm hid} = 10^9$ GeV. The messenger is coupled to A_2 and the flow is taken along the u_1 (left dyon) singularity. We have rescaled $\mu \to (10^9/\tilde{M}_{\rm hid})\mu$, with the hidden scale before rescaling $\tilde{M}_{\rm hid} = 0.2$. We have chosen $M_{\rm m} = 10^{13}$ GeV and $\tan\beta = 10$.

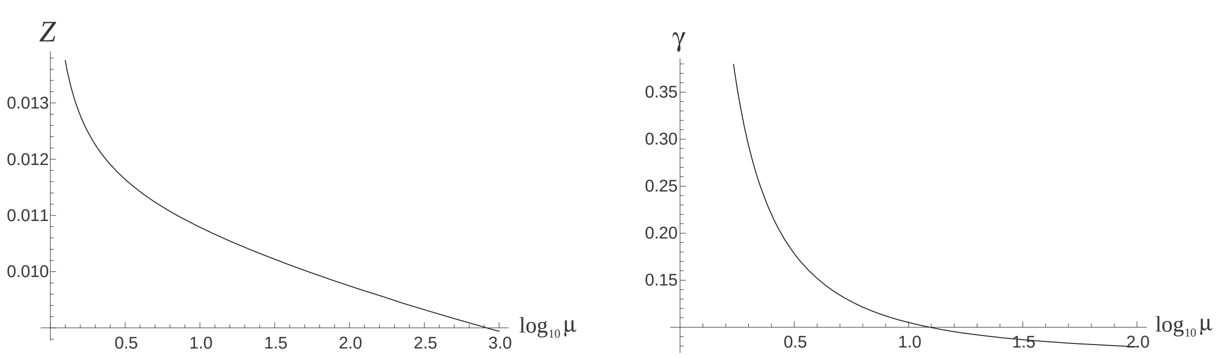

FIG. 10: The wave function renormalization coefficient $Z = b_{22}$ (left) and the anomalous dimension γ (right) along the flow u_2 in the A_2-coupled model.

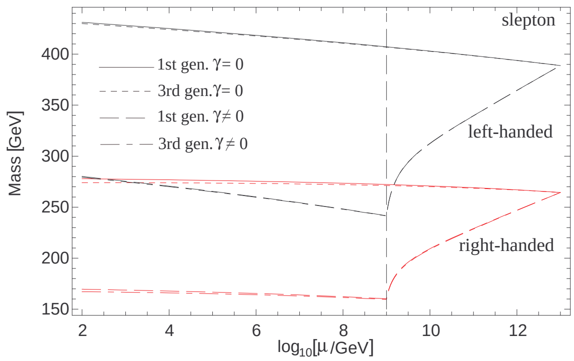

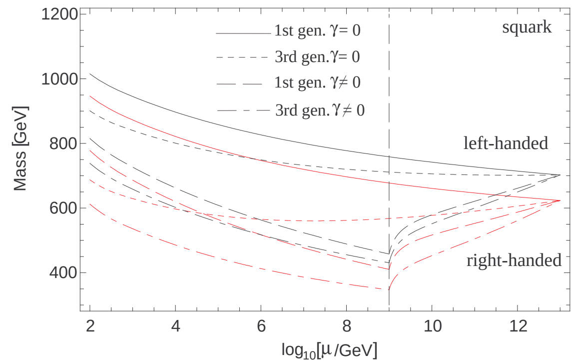

FIG. 11: The mass RG flows for the 1st and 3rd generation sleptons (the left panel) and squarks (right panel), with ($\gamma \neq 0$) and without ($\gamma = 0$) hidden sector effects. The vertical dashed line indicates the hidden scale $M_{\rm hid} = 10^9$ GeV. The messenger is coupled to A_2 and the flow is taken along the u_2 (right dyon) singularity. We have rescaled $\mu \to (10^9/\tilde{M}_{\rm hid})\mu$, with the hidden scale before rescaling $\tilde{M}_{\rm hid} = 1.2$. We have chosen $M_{\rm m} = 10^{13}$ GeV and $\tan\beta = 10$.

the hidden scale to be $\tilde{M}_{\rm hid} = 1.2$ so that the dynamics around the AD point $\mu = 1$ does not contribute to the mass RG flow. The wave function renormalization coefficient and the anomalous dimension,

$$Z_{A_2} = b_{22}(u_2(a_1), a_1)\Big|_{a_1=\mu}, \tag{64}$$

$$\gamma_{A_2} = -2a_1 \frac{d}{da_1} Z_{A_2}(u_2(a_1), a_1)\Big|_{a_1=\mu}, \tag{65}$$

above $\tilde{M}_{\rm hid} = 1.2$ are shown in Fig.10. In this case, the anomalous dimension rapidly increases as the scale approaches $\tilde{M}_{\rm hid}$ from a higher scale. Numerical solutions to the RG equations (42)-(48), with rescaling $\mu \to (10^9/\tilde{M}_{\rm hid})\mu$, are shown in Fig.11. We see that both slepton and squark masses are decreased as the scale goes down from $M_{\rm m}$ to $\tilde{M}_{\rm hid}$. We observe sharp decline of the mass RG flow near $\tilde{M}_{\rm hid}$, which is expected from the behavior of the anomalous dimension.

In the numerical study we chose $\tilde{M}_{\rm hid} = 1.2$ in order to avoid the AD point where the local effective theory description becomes unreliable. If we nevertheless take $\tilde{M}_{\rm hid}$ close to the AD point and take the results at face value, we have extremely large anomalous dimension and very steep decline of the mass RG flow. If this is indeed the case it is phenomenologically very interesting, since the lightest scalar tau (stau) can easily be lighter than the bino, leading to rich implications in collider physics [4]. Furthermore, with the large anomalous dimension one may possibly solve the μ problem of the GMSB scenario [22, 23]. While a reliable effective theory at the AD point is lacking at the moment, it would certainly be worthwhile investigating these possibilities further.

In the present setting with $\tilde{M}_{\rm hid} = 1.2$ and $\tan\beta = 10$, we have the stau mass $m_{\tilde{\tau}} = 167.8$ GeV and the bino mass $M_1 = 134.9$ GeV at the low energy. We find that the stau can be lighter than the bino with moderate values of $\tan\beta$: with $\tan\beta = 25$, for example, we have stau mass $m_{\tilde{\tau}} = 132.9$ GeV and bino mass $M_1 = 134.9$ GeV.

V. SUMMARY AND DISCUSSIONS

In this paper we discussed how a strongly coupled hidden sector dynamics may affect the MSSM low energy mass spectrum, using a calculable model of hidden sector and the minimal GMSB scenario as a concrete example. We found that the effects on the RG flow are qualitatively different from the perturbative toy model cases discussed in [3, 4]. In our strongly coupled example the hidden sector effects can make the scalar masses larger or smaller, depending sensitively on the coupling of the messenger fields to the hidden sector fields, as well as on the dynamics of the hidden sector itself; this is in a stark contrast to the perturbative case where the scalar masses can only be smaller. In fact, this feature is not quite surprising since non-abelian gauge fields have different RG behavior than scalar fields or abelian gauge fields. We expect our finding to be generic in strongly coupled hidden sector models.

Let us touch upon some phenomenological implications of the A_1- and A_2-coupled examples given in Sec.III B. These two models are actually quite different. In the A_1-coupled model (53) the gravitino mass is

$$m_{3/2} \sim \frac{\langle F_{A_1} \rangle}{\sqrt{3} M_{\rm Pl}}, \tag{66}$$

which is $m_{3/2} \sim 1$ GeV with our parameter values ($M_{\rm Pl} = 2.4 \times 10^{18}$ GeV is the reduced Planck mass). The gravitino of this mass is the lightest superparticle (LSP) and it is a good candidate of cold dark matter. For typical neutralino mass range of a few hundred GeV, this gravitino mass is marginally compatible with the Big-Bang nucleosynthesis (BBN) bound [24]. In the A_2-coupled model (54) on the other hand, the gravitino mass is evaluated as

$$m_{3/2} \sim \frac{\langle F_{A_2}\rangle}{\sqrt{3}M_{\rm Pl}} = \frac{M_{\rm c}}{\Lambda}\frac{\langle F_X\rangle}{\sqrt{3}M_{\rm Pl}} \sim \frac{M_{\rm c}}{\Lambda}\times(1\ {\rm GeV}), \quad (67)$$

where $\sqrt{\langle F_X\rangle} \sim 10^9$ GeV is assumed. If $M_{\rm c}/\Lambda \gtrsim \mathcal{O}(100)$, the gravitino cannot be the LSP anymore and in this case, the usual neutralino LSP scenario is applicable. For the parameter set in Fig.10, we have $m_{3/2} \sim 1$ TeV.

Finally, the RG analysis presented in this paper is also possible for other models of strongly coupled hidden sector, as long as they are of perturbed Seiberg-Witten type and the Kähler metric is calculable. The hidden sector RG provides a test bed for studying dynamics of the hidden sector and the mechanism of SUSY breaking on observational basis, and it is certainly very interesting to discuss phenomenological implications of various hidden sector models.

Acknowledgments

M. A. and S. K. thank the organizers of the YITP workshop YITP-W-08-04 on “Development of Quantum Field Theory and String Theory.” This work was supported in part by the Research Program MSM6840770029, the Project of International Cooperation ATLAS-CERN of the Ministry of Education, Youth and Sports of the Czech Republic (M. A.), the WCU grant R32-2008-000-10130-0 (S. K.), and by the DOE Grant #DE-FG02-10ER41714 (N. O.).

Appendix A: $\mathcal{N}=2$ technicalities

In this Appendix we give technical details of the $\mathcal{N}=2$ supersymmetric QCD that are used in actual computations of the hidden sector [12, 13]. A basic assumption on our hidden sector model described in Sec.II C is that the FI term parameter λ is much smaller than the $SU(2)$ dynamical scale Λ and the Landau pole Λ_L is much larger than the $SU(2)$ dynamical scale, namely,

$$\lambda^2 \ll \Lambda \ll \Lambda_L. \quad \text{(A1)}$$

This implies that the FI term is treated as perturbation, and that the $U(1)$ gauge coupling is always weak in scales below the Landau pole $a_1 < \Lambda_L$ so the $SU(2)$ coupling is not affected by the $U(1)$ dynamics. Then the analytic properties of the $\mathcal{N}=2$ $SU(2)$ gauge theory is not spoiled by the FI term nor by the $U(1)$ part.

Below we consider only the supersymmetric part of the action $\mathcal{L}_{\rm SUSY} = \mathcal{L}_{\rm VM} + \mathcal{L}_{\rm HM}$, assuming that the FI term is negligible. We shall focus on the Coulomb branch. The vector multiplet scalars a_2, a_1 and their dual variables a_{2D}, a_{1D} undergo $Sp(4,\mathbb{R})$ duality transformation [8]. The subgroup of $Sp(4,\mathbb{R})$ that leaves the action invariant is in the form [9, 10]:

$$\begin{pmatrix} a_{2D} \\ a_2 \\ a_{1D} \\ a_1 \end{pmatrix} \mapsto \begin{pmatrix} \alpha & \beta & 0 & p \\ \gamma & \delta & 0 & q \\ p\gamma - q\alpha & p\delta - q\beta & 1 & -pq \\ 0 & 0 & 0 & 1 \end{pmatrix} \begin{pmatrix} a_{2D} \\ a_2 \\ a_{1D} \\ a_1 \end{pmatrix}, \quad \text{(A2)}$$

where

$$\begin{pmatrix} \alpha & \beta \\ \gamma & \delta \end{pmatrix} \in SL(2,\mathbb{Z}) \quad \text{(A3)}$$

and $p, q \in \mathbb{Q}$. A crucial observation here is that the (a_{2D}, a_2, a_1) part of the monodromy transformations is identical to that of the $\mathcal{N}=2$ supersymmetric QCD with gauge group $SU(2)$ and two massive hypermultiplets, where the masses are taken to be $m_1 = m_2 = \sqrt{2}a_1$. This is consistent with our assumption that the $SU(2)$ gauge dynamics is intact. The prepotential implied by the monodromy transformation naturally contains the prepotential of the $\mathcal{N}=2$ supersymmetric QCD [8] with $N_f = 2$ massive hypermultiplets and gauge group $SU(2)$,

$$\mathcal{F}(A_2, A_1, \Lambda, \Lambda_L) = \mathcal{F}^{\rm SW}_{SU(2)}(A_2, m_1, m_2, \Lambda)\Big|_{m_1=m_2=\sqrt{2}A_1} + \frac{1}{2}CA_1^2. \quad \text{(A4)}$$

The first term is the supersymmetric QCD part, and the second is a $U(1)$ contribution where the parameter C is determined by the relative scale between Λ_L and Λ.

The periods a_2 and a_{2D} are obtained from the elliptic curve of the $\mathcal{N}=2$ supersymmetric QCD with two massive hypermultiplets,

$$y^2 = \left(x^2 - \frac{\Lambda^4}{64}\right)(x-u) + \frac{1}{4}m_1 m_2 \Lambda^2 x - \frac{\Lambda^4}{64}(m_1^2 + m_2^2), \quad \text{(A5)}$$

where $u = \mathrm{Tr}\,A_2^2$, and $m_1 = m_2 = \sqrt{2}a_1$ now. The Seiberg-Witten differential is

$$\lambda_{\rm SW} = -\frac{\sqrt{2}}{4\pi}\frac{y dx}{x^2 - \frac{1}{64}\Lambda^4}, \quad \text{(A6)}$$

and the periods are given by the contour integrals,

$$a_{2D} = \oint_{\gamma_1} \lambda_{\rm SW}, \quad a_2 = \oint_{\gamma_2} \lambda_{\rm SW}. \quad \text{(A7)}$$

The cycles γ_1, γ_2 are to be specified below. It is convenient to change the variables as $x = 4X + \frac{1}{3}u$ and $y = 4Y$ so that the curve (A5) is uniformized in the Weierstrass form,

$$Y^2 = 4X^3 - g_2 X - g_3 = 4(X-e_1)(X-e_2)(X-e_3), \quad \text{(A8)}$$

with

$$\begin{aligned} g_2 &= \frac{1}{16}\left(\frac{4}{3}u^2 + \frac{\Lambda^4}{16} - 2a_1^2\Lambda^2\right), \\ g_3 &= \frac{1}{16}\left(\frac{a_1^2\Lambda^4}{16} - \frac{a_1^2\Lambda^2}{6}u - \frac{\Lambda^4}{96}u + \frac{2}{27}u^3\right), \end{aligned} \quad \text{(A9)}$$

and the three roots are

$$\begin{aligned} e_1 &= \frac{u}{24} - \frac{\Lambda^2}{64} - \frac{1}{8}\sqrt{(u+\frac{\Lambda^2}{8})^2 - 2a_1^2\Lambda^2}, \\ e_2 &= \frac{u}{24} - \frac{\Lambda^2}{64} + \frac{1}{8}\sqrt{(u+\frac{\Lambda^2}{8})^2 - 2a_1^2\Lambda^2}, \\ e_3 &= -\frac{u}{12} + \frac{\Lambda^2}{32}. \end{aligned} \tag{A10}$$

The three singular points (30) arise when two of these roots coincide. With the change of variables the Seiberg-Witten differential becomes

$$\lambda_{\rm SW} = \frac{\sqrt{2}}{4\pi}\frac{dX}{Y}\left(\frac{2}{3}u - 4X - \frac{1}{8}\frac{a_1^2\Lambda^2}{X-c}\right), \tag{A11}$$

with

$$c = -\frac{u}{12} - \frac{\Lambda^2}{32}. \tag{A12}$$

The contours of the integrals (A7) are fixed by the asymptotic behavior of the periods,

$$a_{2D} \sim \frac{i}{2\pi}\sqrt{2u}\ln\frac{u}{\Lambda^2}, \quad a_2 \sim \frac{\sqrt{2u}}{2}, \tag{A13}$$

in the region $u \to \infty$; the correct contours turn out to be that γ_1 encircles $\{e_2, e_3\}$ and γ_2 encircles $\{e_1, e_3\}$. The periods are now expressed as

$$a_{2D} = \frac{\sqrt{2}}{4\pi}\left(\frac{4}{3}uI_1^{(1)} - 8I_2^{(1)} - \frac{a_1^2\Lambda^2}{4}I_3^{(1)}(c)\right), \tag{A14}$$

$$a_2 = \frac{\sqrt{2}}{4\pi}\left(\frac{4}{3}uI_1^{(2)} - 8I_2^{(2)} - \frac{a_1^2\Lambda^2}{4}I_3^{(2)}(c)\right) + a_1, \tag{A15}$$

using integrals

$$\begin{aligned} I_1^{(i)} = \frac{1}{2}\oint_{\gamma_i}\frac{dX}{Y}, \qquad I_2^{(i)} = \frac{1}{2}\oint_{\gamma_i}\frac{XdX}{Y}, \\ I_3^{(i)}(c) = \frac{1}{2}\oint_{\gamma_i}\frac{dX}{Y(X-c)}. \end{aligned} \tag{A16}$$

It is convenient to express the integrals using the Weierstrass functions through the Abel-Jacobi map:

$$(\wp(z), \wp'(z)) \mapsto (X, Y). \tag{A17}$$

This is a map from $\mathbb{C}/\Gamma$ to the curve (A8), where Γ is the lattice spanned by periods ω_1 and ω_2. The Weierstrass σ, ζ, and $\wp$ functions are

$$\begin{aligned} \sigma(z) = z\prod_{w\in\Gamma^*}\left(1-\frac{z}{w}\right)\exp\left\{\frac{z}{w} + \frac{1}{2}\left(\frac{z}{w}\right)^2\right\}, \\ \zeta(z) = \frac{d\ln\sigma(z)}{dz}, \qquad \wp(z) = -\frac{d\zeta(z)}{dz}, \end{aligned} \tag{A18}$$

where $\Gamma^* = \Gamma - \{0\}$. The function $\wp(z)$ is even whereas $\zeta(z)$ and $\sigma(z)$ are odd. Introducing $\omega_3 = -\omega_1 - \omega_2$, the half periods are related to the three roots (A10) as $e_i = \wp(\omega_i/2)$, $i = 1, 2, 3$. Denoting also $\eta_i = \zeta(\frac{\omega_i}{2})$, the following relations are well known:

$$e_1 + e_2 + e_3 = 0, \tag{A19}$$

$$\eta_1 + \eta_2 + \eta_3 = 0, \tag{A20}$$

$$\omega_1\eta_2 - \omega_2\eta_1 = \omega_2\eta_3 - \omega_3\eta_2 = \omega_3\eta_1 - \omega_1\eta_3 = \pi i. \tag{A21}$$

The last identities are known as Legendre's relations. Following relations are also well known:

$$\frac{\wp'(z_0)}{\wp(z) - \wp(z_0)} = 2\zeta(z_0) - \zeta(z+z_0) - \zeta(z-z_0), \tag{A22}$$

$$\sigma(z+\omega_i) = -\sigma(z)\exp[\eta_i(2z+\omega_i)]. \tag{A23}$$

The inverse of (A17) is

$$z = \int_\infty^p \frac{dX}{Y} = -\frac{1}{\sqrt{e_2 - e_1}}F(\phi, k), \tag{A24}$$

where $F(\phi, k)$ is the incomplete elliptic integral of the first kind and $k^2 = (e_3 - e_1)/(e_2 - e_1)$, $\sin^2\phi = (e_2 - e_1)/(p - e_1)$. The integrals (A16) are expressed using the Weierstrass functions as $(i = 1, 2)$

$$I_1^{(i)} = \int_{\frac{\omega_{3-i}}{2}}^{-\frac{\omega_3}{2}} dz = \frac{1}{2}\omega_i, \tag{A25}$$

$$I_2^{(i)} = \int_{\frac{\omega_{3-i}}{2}}^{-\frac{\omega_3}{2}} \wp(z)dz = -\eta_i, \tag{A26}$$

$$I_3^{(i)}(c) = \int_{\frac{\omega_{3-i}}{2}}^{-\frac{\omega_3}{2}} \frac{dz}{\wp(z) - \wp(z_0)} = \frac{\omega_i\zeta(z_0) - 2\eta_i z_0}{\wp'(z_0)}, \tag{A27}$$

where z_0 is the point on $\mathbb{C}/\Gamma$ such that $X = \wp(\pm z_0) = c$, $Y = \wp'(\pm z_0) = \pm i a_1\Lambda^2/8\sqrt{2}$.

Below we describe a way of computing the matrix [9, 12, 13],

$$\tau_{ij} = \frac{\partial^2\mathcal{F}}{\partial a_i\partial a_j} = \frac{\partial a_{iD}}{\partial a_j}. \tag{A28}$$

The computation of τ_{22} is straightforward. We have

$$\tau_{22} = \left.\frac{\partial a_{2D}}{\partial a_2}\right|_{a_1} = \left.\frac{\partial a_{2D}}{\partial u}\right|_{a_1}\left.\frac{\partial u}{\partial a_2}\right|_{a_1} = \frac{I_1^{(1)}}{I_1^{(2)}} = \frac{\omega_1}{\omega_2}. \tag{A29}$$

Similarly,

$$\begin{aligned} \tau_{21} = \left.\frac{\partial a_{2D}}{\partial a_1}\right|_{a_2} &= \left.\frac{\partial a_{2D}}{\partial a_1}\right|_{u} - \tau_{22}\left.\frac{\partial a_2}{\partial a_1}\right|_{u} \\ &= -\frac{\sqrt{2}\Lambda^2 a_1}{16\pi}\left(I_3^{(1)}(c) - \frac{\omega_1}{\omega_2}I_3^{(2)}(c)\right) - \tau_{22} \\ &= -\frac{2z_0}{\omega_2} - \tau_{22}, \end{aligned} \tag{A30}$$

where (A21) and (A27) have been used. For computing τ_{11} we start with the Euler relation,

$$2\mathcal{F} = a_1 a_{1D} + a_2 a_{2D} + \Lambda\frac{\partial\mathcal{F}}{\partial\Lambda}, \tag{A31}$$

which follows from the fact that the $\mathcal{N}=2$ prepotential is a homogeneous function of degree 2. The last term is proportional to the 1-loop beta function [25–28] and in our case of color $N_c=2$ and flavor $N_f=2$,

$$\Lambda\frac{\partial\mathcal{F}}{\partial\Lambda}=\frac{2N_c-N_f}{4\pi i}u=\frac{u}{2\pi i}. \tag{A32}$$

Differentiating (A31) with respect to a_1 one obtains,

$$a_{1D}=a_1\tau_{11}+a_2\tau_{21}-\frac{1}{2\pi i}\left.\frac{\partial u}{\partial a_2}\right|_{a_1}\left.\frac{\partial a_2}{\partial a_1}\right|_{u}. \tag{A33}$$

On the RHS,

$$\begin{aligned}\left.\frac{\partial u}{\partial a_2}\right|_{a_1} &= \left(\left.\frac{\partial a_2}{\partial u}\right|_{a_1}\right)^{-1}=\frac{8\pi}{\sqrt{2}\omega_2}, &\text{(A34)}\\ \left.\frac{\partial a_2}{\partial a_1}\right|_{u} &= -\frac{\sqrt{2}a_1\Lambda^2}{16\pi}I_3^{(2)}(c)+1, &\text{(A35)}\end{aligned}$$

and a_2 is (A15) with the integrals given by (A25), (A26), (A27). In order to evaluate a_{1D} on the LHS, we use the reciprocity law [29] for differentials of the first kind (a holomorphic 1-form) χ, and the third kind (a meromorphic form with single poles) ψ, on a genus one Riemann surface,

$$\oint_{\gamma_2}\chi\oint_{\gamma_1}\psi-\oint_{\gamma_1}\chi\oint_{\gamma_2}\psi=2\pi i\sum_n\left(\mathrm{Res}_{x_n^+}\psi\right)\int_{x_n^-}^{x_n^+}\chi, \tag{A36}$$

where x_n^+ and x_n^- are the poles on the positive and negative Riemann sheets. Applying this to $\chi=\partial\lambda_{\rm SW}/\partial a_2|_{a_1}$ and $\psi=\partial\lambda_{\rm SW}/\partial a_1|_u$, we have

$$\begin{aligned}\left.\frac{\partial a_{1D}}{\partial a_2}\right|_{a_1} &= \left.\frac{\partial a_{2D}}{\partial a_1}\right|_{u}-\left.\frac{\partial a_{2D}}{\partial a_2}\right|_{a_1}\left.\frac{\partial a_2}{\partial a_1}\right|_{u}\\ &= -\int_{x_0^-}^{x_0^+}\left.\frac{\partial\lambda_{SW}}{\partial a_2}\right|_{a_1}, &\text{(A37)}\end{aligned}$$

where $x_0^\pm=\wp(\pm z_0)$ on the two Riemann sheets for the point $X=c$. Integrating, we obtain

$$a_{1D}=-\int_{x_0^-}^{x_0^+}\lambda_{SW}+\tilde{C}(a_1), \tag{A38}$$

with $\tilde{C}(a_1)$ the constant of integration. The integral can be expressed using the Weierstrass functions as

$$\begin{aligned}\int_{x_0^-}^{x_0^+}\frac{dX}{Y} &= \int_{-z_0}^{z_0}dz=2z_0, &\text{(A39)}\\ \int_{x_0^-}^{x_0^+}\frac{XdX}{Y} &= \int_{-z_0}^{z_0}\wp(z)dz=-2\zeta(z_0), &\text{(A40)}\\ \int_{x_0^-}^{x_0^+}\frac{dX}{Y(X-c)} &= \int_{-z_0-\epsilon}^{z_0+\epsilon}\frac{dz}{\wp(z)-\wp(z_0)}\\ &= \frac{2}{\wp'(z_0)}\left[2z_0\zeta(z_0)-\ln\sigma(2z_0)+\ln\sigma(\epsilon)\right], &\text{(A41)}\end{aligned}$$

where the last integral is divergent and the regulator ϵ has been introduced. It is possible to pass on the divergence to the integration constant and $\tilde{C}(a)$ is now related to C of (A4) as $\tilde{C}(a_1)=a_1(C+\frac{i}{\pi}\ln\sigma(\epsilon))$. Inserting these expressions into (A33) we finally obtain,

$$\tau_{11}=\frac{i}{\pi}\left(\ln\sigma(2z_0)-4z_0^2\frac{\eta_2}{\omega_2}\right)-2\tau_{21}-\tau_{22}+C. \tag{A42}$$

In the numerical computations we have set $C=8\pi i$ which corresponds to $\Lambda_L/\Lambda\sim10^{17-18}$.

[1] M. Dine et al., Phys. Rev. **D70**, 045023 (2004), hep-ph/0405159.
[2] A. G. Cohen, T. S. Roy, and M. Schmaltz, JHEP **02**, 027 (2007), hep-ph/0612100.
[3] B. A. Campbell, J. Ellis, and D. W. Maybury (2008), 0810.4877.
[4] M. Arai, S. Kawai, and N. Okada, Phys. Rev. **D81**, 035022 (2010), 1001.1509.
[5] E. Witten, Phys. Lett. **B105**, 267 (1981).
[6] M. Dine, W. Fischler, and M. Srednicki, Nucl. Phys. **B189**, 575 (1981); S. Dimopoulos and S. Raby, Nucl. Phys. **B192**, 353 (1981); L. Alvarez-Gaume, M. Claudson, and M. B. Wise, Nucl. Phys. **B207**, 96 (1982); M. Dine and W. Fischler, Nucl. Phys. **B204**, 346 (1982); C. R. Nappi and B. A. Ovrut, Phys. Lett. **B113**, 175 (1982); M. Dine and A. E. Nelson, Phys. Rev. **D48**, 1277 (1993), hep-ph/9303230; M. Dine, A. E. Nelson, and Y. Shirman, Phys. Rev. **D51**, 1362 (1995), hep-ph/9408384; M. Dine, A. E. Nelson, Y. Nir, and Y. Shirman, Phys. Rev. **D53**, 2658 (1996), hep-ph/9507378.
[7] N. Seiberg and E. Witten, Nucl. Phys. **B426**, 19 (1994), hep-th/9407087.
[8] N. Seiberg and E. Witten, Nucl. Phys. **B431**, 484 (1994), hep-th/9408099.
[9] L. Alvarez-Gaume, M. Marino, and F. Zamora, Int. J. Mod. Phys. **A13**, 403 (1998), hep-th/9703072.
[10] L. Alvarez-Gaume, M. Marino, and F. Zamora, Int. J. Mod. Phys. **A13**, 1847 (1998), hep-th/9707017.
[11] A. Bilal and F. Ferrari, Nucl. Phys. **B516**, 175 (1998), hep-th/9706145.
[12] M. Arai and N. Okada, Phys. Rev. **D64**, 025024 (2001), hep-th/0103157.

[13] M. Arai, C. Montonen, N. Okada, and S. Sasaki, Phys. Rev. **D76**, 125009 (2007), 0708.0668.
[14] P. Fayet, Nucl. Phys. **B113**, 135 (1976).
[15] L. Alvarez-Gaume and M. Marino, Int. J. Mod. Phys. **A12**, 975 (1997), hep-th/9606191.
[16] S. R. Coleman, Phys. Rev. **D15**, 2929 (1977).
[17] C. G. Callan, Jr. and S. R. Coleman, Phys. Rev. **D16**, 1762 (1977).
[18] M. J. Duncan and L. G. Jensen, Phys. Lett. **B291**, 109 (1992).
[19] D. J. Castano, E. J. Piard, and P. Ramond, Phys. Rev. **D49**, 4882 (1994), hep-ph/9308335.
[20] E. Gildener and S. Weinberg, Phys. Rev. **D13**, 3333 (1976).
[21] M. Sher, Phys. Rept. **179**, 273 (1989).
[22] T. S. Roy and M. Schmaltz, Phys. Rev. **D77**, 095008 (2008), 0708.3593.
[23] H. Murayama, Y. Nomura, and D. Poland, Phys. Rev. **D77**, 015005 (2008), 0709.0775.
[24] M. Kawasaki, K. Kohri, T. Moroi, and A. Yotsuyanagi, Phys. Rev. **D78**, 065011 (2008), 0804.3745.
[25] M. Matone, Phys. Lett. **B357**, 342 (1995), hep-th/9506102.
[26] J. Sonnenschein, S. Theisen, and S. Yankielowicz, Phys. Lett. **B367**, 145 (1996), hep-th/9510129.
[27] T. Eguchi and S.-K. Yang, Mod. Phys. Lett. **A11**, 131 (1996), hep-th/9510183.
[28] E. D'Hoker, I. M. Krichever, and D. H. Phong, Nucl. Phys. **B494**, 89 (1997), hep-th/9610156.
[29] J. H. Phillip Griffiths, *Principles of Algebraic Geometry* (Wiley-Interscience, 1994).